© 2018. Published by The Company of Biologists Ltd | Development (2018) 145, dev163519. doi:10.1242/dev.163519

RESEARCH ARTICLE

Molecular analysis of enthesopathy in a mouse model of hypophosphatemic rickets

Eva S. Liu[1,2,3], Janaina S. Martins[2,3], Wanlin Zhang[2] and Marie B. Demay[2,3,*]

ABSTRACT

The bone tendon attachment site known as the enthesis comprises a transitional zone between bone and tendon, and plays an important role in enabling movement at this site. X-linked hypophosphatemia (XLH) is characterized by impaired activation of vitamin D, elevated serum FGF23 levels and low serum phosphate levels, which impair bone mineralization. Paradoxically, an important complication of XLH is mineralization of the enthesis (enthesopathy). Studies were undertaken to identify the cellular and molecular pathways important for normal post-natal enthesis maturation and to examine their role during the development of enthesopathy in mice with XLH (Hyp). The Achilles tendon entheses of Hyp mice demonstrate an expansion of hypertrophic-appearing chondrogenic cells by P14. Post-natally, cells in wild-type and Hyp entheses similarly descend from scleraxis- and Sox9-expressing progenitors; however, Hyp entheses exhibit an expansion of Sox9-expressing cells, and enhanced BMP and IHH signaling. These results support a role for enhanced BMP and IHH signaling in the development of enthesopathy in XLH.

KEY WORDS: Enthesis, Tendon-bone attachment, XLH, BMP, IHH, 1,25 dihydroxyvitamin D, Phosphate, FGF23

INTRODUCTION

The enthesis is a specialized tissue that forms at the site of attachment of tendon to bone, optimizing the transfer of mechanical stress and force from muscle to bone, allowing for limb and body movement (Zelzer et al., 2014). The fibrocartilaginous transitional zone between bone and tendon consists of four zones, including the bony eminence, mineralized fibrocartilage, unmineralized fibrocartilage and tendon (Zelzer et al., 2014). This region is characterized by a gradual increase in mineral content and a characteristic distribution of collagens and proteoglycans (Genin et al., 2009; Schwartz et al., 2012).

The bHLH transcription factor scleraxis (Scx), a specific marker for tendon and ligament progenitors, is required for formation of force-transmitting and intermuscular tendons, as well as a functional enthesis (Schweitzer et al., 2001; Murchison et al., 2007; Killian and Thomopoulos, 2016). During embryonic development, the bony eminence into which tendons insert expresses both *Scx* and *Sox9*, the latter of which is a BMP target gene that marks chondroprogenitor cells during endochondral bone formation (Bi et al., 1999); however, the cells closest to bone are more likely to arise from Sox9$^+$ progenitors (Akiyama et al., 2005; Sugimoto et al., 2013). The BMP pathway has been implicated in inducing chondrocyte cell fate during development of the deltoid tuberosity into which tendons insert (Minina et al., 2001; Kumar et al., 2012). Consistent with this, factors that regulate chondrocyte differentiation, including Indian hedgehog (IHH) and its receptor patched 1 (PTCH1), are expressed in the enthesis (Chen et al., 2006; Thomopoulos et al., 2010; Liu et al., 2012). Of note, IHH which is secreted by prehypertrophic and early hypertrophic chondrocytes (St-Jacques et al., 1999; Kronenberg, 2003), has been implicated in the pathogenesis of pathological ligament ossification (Sugita et al., 2013).

X-linked hypophosphatemia (XLH) is the most common form of hypophosphatemic rickets, with an incidence of 1:20,000 in the general population (Carpenter et al., 2011). It is characterized by a mutation in PHEX, leading to elevated serum FGF23 levels, hypophosphatemia and suppression of the vitamin D 1-alpha-hydroxylase (Holm et al., 1997; Jonsson et al., 2003; Liu et al., 2006). This results in rickets and impaired mineralization of bone. A significant complication of XLH in adults is the paradoxical mineralization of the tendon-bone attachment site (enthesopathy), which results in pain, impaired movement and decreased quality of life (Liang et al., 2009). The molecular and cellular basis of the enthesopathy in XLH is poorly understood. Therefore, studies in the murine model of XLH (Hyp) were undertaken to address the origin of aberrant cells that give rise to the enthesopathy, as well as to identify roles for BMP and IHH signaling pathways in the pathogenesis of enthesopathy. As previous studies have focused on normal enthesis development during embryogenesis, these studies also provide insight into the molecular and cellular pathways involved in normal postnatal enthesis maturation.

RESULTS

Wild-type and Hyp enthesis cells orginate from Sox9$^+$ and Scx$^+$ cells

Previous studies have demonstrated an expansion of fibrocartilage in the Achilles tendon entheses of P30 Hyp mice (Liang et al., 2009). To determine the time at which enthesopathy first develops, the presence of proteoglycans characteristic of chondrocyte matrix was evaluated by Safranin O staining of the Achilles tendon entheses of wild-type and Hyp mice P7, P14, P30 and P60 (Fig. 1). The Achilles enthesis of P14 wild-type mice is characterized by sparse hypertrophic-appearing cells and a paucity of SafO$^+$ matrix; by P30, both the SafO$^+$ matrix and hypertrophic-appearing cells are absent. Although the Hyp entheses are normal at P7, with Safranin O-staining matrix (SafO$^+$) limited to the calcaneal secondary ossification center, hypertrophic-appearing cells and SafO$^+$ matrix are present in the Achilles enthesis by P14, extending towards the tendon at P30 and P60 (Fig. 1). This abnormal expansion of hypertrophic-appearing cells in Hyp entheses will be referred to as hypertrophic enthesopathy cells (HECs).

During embryonic development, the enthesis develops from cells expressing the chondrogenic transcription factor Sox9 and Scx, a

[1]Division of Endocrinology, Diabetes, and Hypertension, Brigham and Women's Hospital, Boston, MA 02115, USA. [2]Endocrine Unit, Massachusetts General Hospital, Boston, MA 02114, USA. [3]Harvard Medical School, Boston, MA 02115, USA.

*Author for correspondence (demay@helix.mgh.harvard.edu)

M.B.D., 0000-0001-5845-5479

Received 16 January 2018; Accepted 4 July 2018

Development (2018) 145, dev163519. doi:10.1242/dev.163519

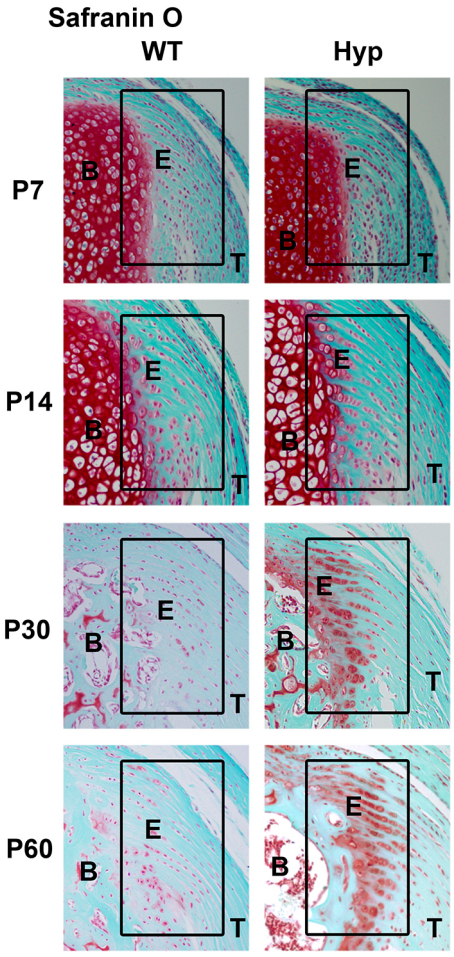

Fig. 1. Hyp entheses exhibit an expansion of Safranin O$^+$ cells. Safranin O staining (red) of wild-type and Hyp entheses. Sections were counterstained with Fast Green. The enthesis region is outlined with a black box (B, bone; E, enthesis; T, tendon). Data are representative of three mice per age/genotype group.

marker of tendon cells, with cells in the embryonic enthesis having been shown to express both Sox9 and Scx (Blitz et al., 2013; Sugimoto et al., 2013). Therefore, lineage-tracing studies were performed to determine whether the cells in the wild-type postnatal enthesis and the HECs descend from Sox9$^+$, Scx$^+$ or Sox9$^+$/Scx$^+$ progenitors. Sox9-CreERT2: R26R^{Tom}, Scx-Cre:R26R^{Tom} and Scx-CreERT2: R26R^{Tom} mice were generated in the Hyp background. Lineage-tracing studies demonstrate that cells labeled with Scx-Cre populate the entheses of both wild-type and Hyp mice at P30 (Fig. 2A). The percentage of Scx-Tomato-positive cells is similar in wild-type and Hyp entheses (wild type versus Hyp: 75.1±1.9% versus 77.3±4.1%, P>0.05). As the HECs in Hyp entheses appear by P14, induction of Scx-CreERT2 at P2 confirms that P14 wild-type and Hyp enthesis cells are descendants of Scx-expressing cells (Fig. 2B). Because the HECs in Hyp entheses appear postnatally and Sox9 immunoreactive cells are present in the wild-type and Hyp entheses by P2 (Fig. 3A), Sox9-CreERT2 was induced by tamoxifen injection at P2, demonstrating that descendants of Sox9-expressing cells populate the entheses of both wild-type and Hyp mice (Fig. 3B). Although few Sox9-CreERT2 labeled cells are observed in the proximal enthesis at P5, by P14, the entire enthesis and proximal region of the tendon is populated with Sox9-CreERT2-labeled cells; by P30, descendants of these cells populate the entire enthesis and tendon in both wild-type and Hyp mice (Fig. 3B). Thus, these results demonstrate that the HECs in Hyp mice originate from the same population of Scx- and Sox9-expressing progenitors that give rise to the wild-type enthesis.

Hyp entheses are characterized by an expansion of Sox9$^+$ cells

As the cells in the enthesis of wild-type and Hyp mice descend from Sox9$^+$ and Scx$^+$ progenitors, we examined whether expression of chondrocyte markers persists in the pathological HECs. Immunohistochemical analyses demonstrate the presence of Sox9-immunoreactive cells in the entheses of both wild-type and Hyp mice. However, by P30 there is an expansion in the domain of Sox9-expressing HECs in the Hyp entheses (Fig. 4A). In contrast, although cells expressing GFP under the Scx promoter (Scx-GFP) are present in the Achilles tendon entheses of wild-type and Hyp mice at P14, by P30, no Scx-GFP expressing cells are seen in the proximal Achilles tendon enthesis in either wild-type or Hyp mice (Fig. 4B). Immunofluorescent staining for Sox9 confirms the presence of Sox9$^+$/Scx$^+$ cells in the enthesis of both wild-type and Hyp mice P14. However, Sox9 immunoreactivity in the proximal enthesis region persists P30 in Hyp, but not in wild-type mice (Fig. 4B). The expansion of Sox9 immunoreactive cells is evidenced by the significant increase in the percentage of cells immunoreactive for Sox9 in P30 Hyp entheses (wild type versus Hyp: 23.2±2.7% versus 52.1±1.6%, P<0.05). Consistent with the time course of expansion of Safranin O- and Sox9-positive cells in Hyp entheses, alkaline phosphatase activity is not altered in P5 Hyp entheses (data not shown), but is increased in Hyp entheses at P14 and P30 (Fig. 5A). Like Sox9 expression, alkaline phosphatase staining is limited to the distal portion of wild-type entheses, and is expanded in the Hyp entheses. Immunohistochemistry for proliferating cell nuclear antigen (PCNA) demonstrates that the proliferation of enthesis cells decreases by P30, but the percentage of proliferating HECs is similar in wild-type and Hyp mice (Fig. 5B,C). These results suggest that the mineralizing enthesopathy observed in XLH is due to persistence of Sox9-expressing, alkaline phosphatase-positive chondrocytic cells in the enthesis.

BMP and IHH signaling is enhanced in Hyp entheses

Because the HECs have features characteristic of chondrocytes, including expression of Sox9 and presence of Safranin O-stained matrix, signaling pathways that regulate chondrocyte differentiation were examined. BMP signaling induces phosphorylation of Smad1/5/9 and expression of Sox9, promoting chondrocyte hypertrophy (Kobayashi et al., 2005; Kumar et al., 2012). Consistent with enhanced BMP signaling, an expansion of p-Smad1/5/9-immunoreactive cells is observed in P14 Hyp entheses and persists until P30 (Fig. 6A). Although the percentage of immunoreactive p-Smad1/5/9 cells in wild-type and Hyp entheses is not different at P7, an increase is seen in Hyp entheses compared with wild type at P14 and P30 (wild type versus Hyp, P7: 29.4±3.7% versus 29.3±4.5%; P14: 31.2±2.0% versus 57.4±6.6%; P30: 17.4±2.2% versus 44.5±0.5%, P<0.05 for P14 and P30). The BMP target gene IHH is necessary for both normal enthesis fibrocartilage development and chondrocyte maturation (Minina et al., 2001; Seki and Hata, 2004; Liu et al., 2013). Consistent with enhanced IHH signaling, an expansion of HECs expressing the IHH target and receptor, PTCH, is observed in P14 Hyp entheses and persists until P30 (Fig. 6B).

To confirm the enhanced BMP and IHH signaling in Hyp entheses, mRNA expression of BMP and IHH target genes was analyzed in P14 wild-type and Hyp entheses. These studies

Development (2018) 145, dev163519. doi:10.1242/dev.163519

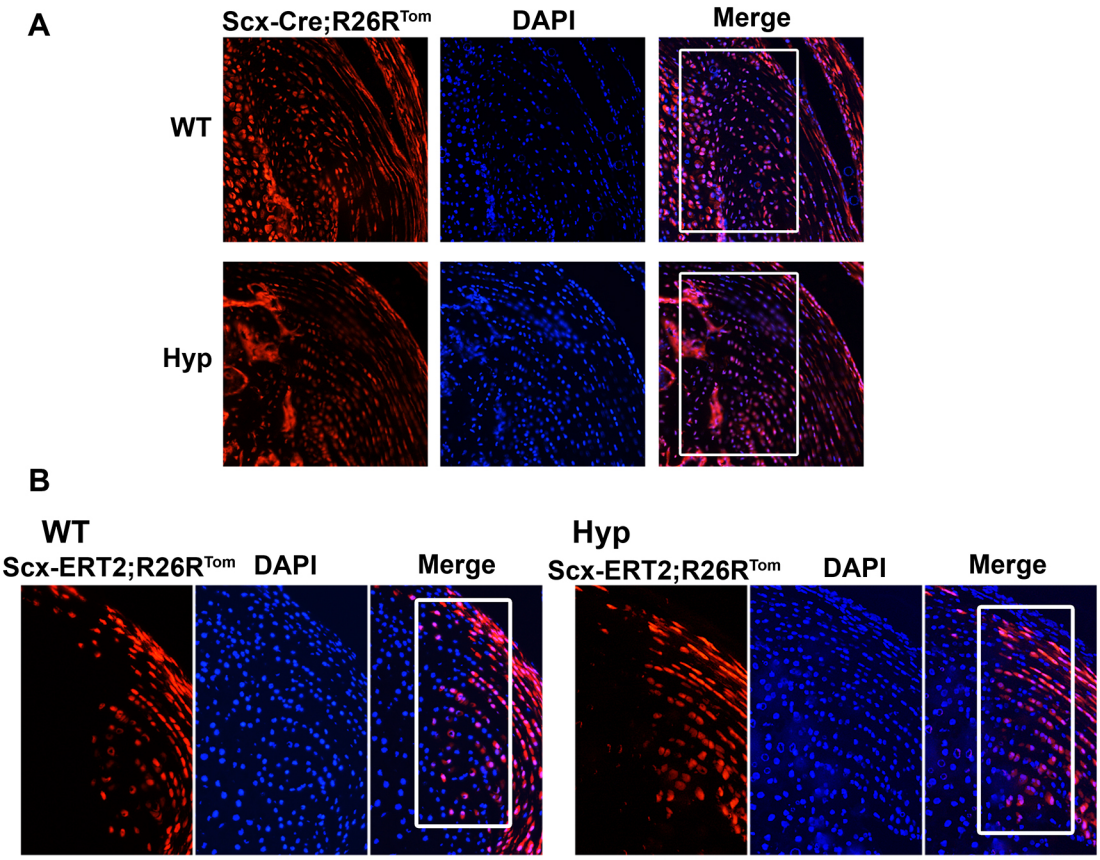

Fig. 2. Hyp enthesopathy cells descend from Scx$^+$ progenitors. (A) Representative images of P30 entheses from Scx-Cre;R26R^{Tom} wild-type and Scx-Cre;R26R^{Tom} Hyp mice. Data are representative of three mice per age/genotype group. (B) Representative images of entheses from Scx-CreERT2;R26R^{Tom} wild-type and Scx-CreERT2;R26R^{Tom} Hyp mice. A single dose of tamoxifen was injected at P2 and mice were sacrificed at P14. Data are representative of at least two mice per age/genotype group.

demonstrate increased expression of the BMP target gene *Nog*, as well as that of *Ihh* and its target genes *Ptch1*, *Runx2* and *Gli1* (Fig. 6C). Expression of *Acan* was also increased in the Hyp entheses. The mRNA expression of *Pgr4*, a marker of articular cartilage, and *Scx*, a marker of tendon, was similar in the wild-type and Hyp entheses, confirming that the entheses analyzed were consistently isolated (Fig. 6C). BMP2 and BMP6 have been implicated in the development of enthesitis in a murine model of ankylosing spondylitis and BMP4 is necessary for the formation of the bony ridge into which the deltoid tendon inserts (Lories et al., 2005; Blitz et al., 2009). Furthermore, enthesis cells are descendants of GDF5$^+$ cells (Dyment et al., 2015). The mRNA expression of GDF5, but not that of BMP2, BMP4 or BMP6, was increased in Hyp entheses relative to wild type, suggesting that increased expression of GDF5 underlies the enhanced BMP signaling in Hyp entheses (Fig. 6D) that promotes aberrant chondrogenesis, leading to enthesopathy.

1,25D and FGF23Ab treatment of Hyp mice attenuates development of enthesopathy

To determine whether hypophosphatemia, impaired 1,25 dihydroxyvitamin D (1,25D) signaling or enhanced FGF23 action contribute to the development of enthesopathy, Hyp mice were treated daily with 1,25D (175 pg/g/day) or three times per week with an FGF23-blocking antibody (FGF23Ab) starting on P2. Both treatments similarly increased serum phosphate levels and maintained normocalcemia (Table 1), consistent with previous reports (Liu et al., 2016). Safranin O staining demonstrates an attenuation of proteoglycans in the entheses of P30 Hyp mice treated with 1,25D or FGF23Ab (Fig. 7A,C). Both treatments decreased p-Smad 1/5/9, Ptch1 and Runx2 immunoreactivity in the Hyp entheses (Fig. 7A,C). These treatments also attenuated alkaline phosphatase activity (Fig. 7B,C).

1,25D suppresses BMP induced IHH signaling in chondrogenic cells

FGF23 impairs activation of vitamin D to 1,25D, thus both 1,25D and FGF23Ab treatment of Hyp mice increase 1,25D signaling (Liu et al., 2016). As they also prevent the development of enthesopathy, it was hypothesized that 1,25D attenuates BMP-induced IHH signaling. As fibrocartilaginous enthesis cells have features of early chondrocytes, primary murine proliferative chondrocytes were treated with rhBMP2 with or without pretreatment with 1,25D. Treatment with rhBMP2 significantly induced the mRNA expression of *Ihh* and its target genes compared with control (Fig. 8). 1,25D pretreatment attenuated BMP induction of *Ihh* and blocked induction of *Ptch* and *Gli1* (Fig. 8). These data implicate impaired 1,25D signaling in the pathogenesis of enthesopathy in XLH.

DISCUSSION

Our results demonstrate that postnatal enthesis maturation recapitulates the development of the embryonic tendon-bone insertion site (Blitz et al., 2013; Sugimoto et al., 2013). Postnatal Achilles tendon enthesis cells of both wild-type and Hyp mice

Development (2018) 145, dev163519. doi:10.1242/dev.163519

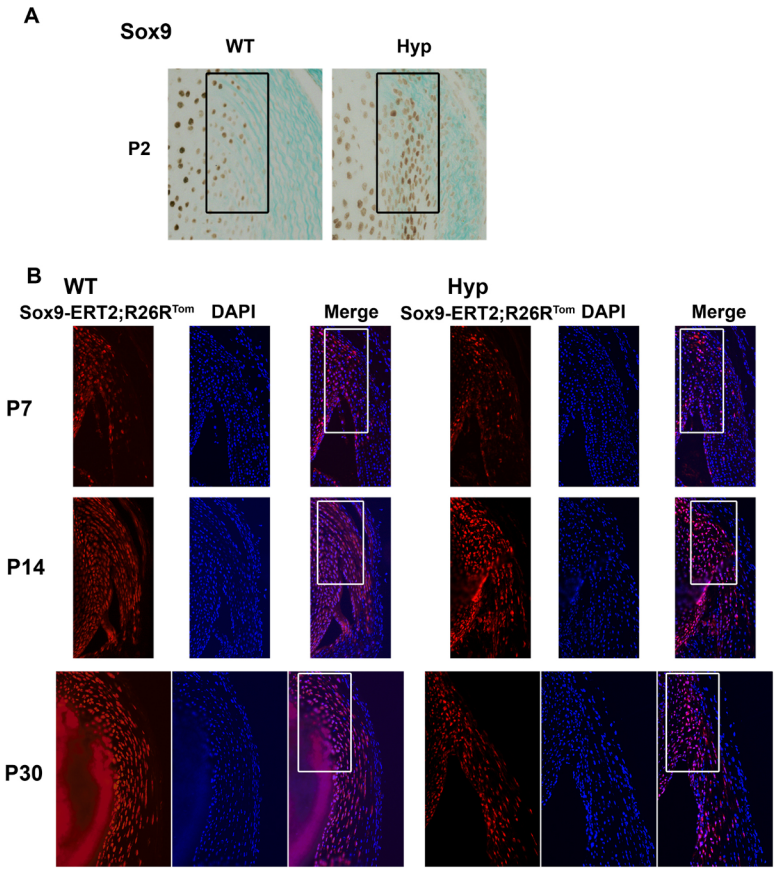

Fig. 3. Hyp enthesopathy cells descend from Sox9-expressing cells. (A) Immunohistochemistry for Sox9 (brown) in P2 wild-type and Hyp entheses. Sections were counterstained with Fast Green. (B) Representative images of entheses from Sox9-CreERT2;R26R^{Tom} wild-type and Sox9-CreERT2;R26R^{Tom} Hyp mice. A single dose of tamoxifen was injected at P2 and mice were sacrificed at P7, P14 and P30. Data are representative of three mice per age/genotype group.

originate from Scx- and Sox9-expressing progenitors, with both Scx and Sox9 being expressed in this region postnatally. These studies also highlight the changing expression pattern of Scx, Sox9 and the IHH target gene *Ptch1* in the normal postnatal maturing fibrocartilaginous enthesis. Expression of these markers in the wild-type enthesis is localized adjacent to the bone up to P14 and is focused more distally, extending to the tendon as the enthesis matures by P30. Consistent with this, lineage-tracing experiments revealed that while Gli1-CreERT2-labeled cells populate the proximal region of the wild-type murine enthesis early in postnatal life up to P13, by P56 the Gli1^{+} cells are limited to the distal region adjacent to the tendon (Schwartz et al., 2015).

The similar staining pattern of p-Smad1/5/9, Ptch1 and Sox9 in wild-type entheses at each age examined indicates that BMP signaling may stimulate IHH signaling in enthesis cells to promote and regulate fibrocartilage formation. In support of this, the current results and previous studies demonstrate that BMP signaling induces IHH signaling in chondrocytes (Grimsrud et al., 2001;

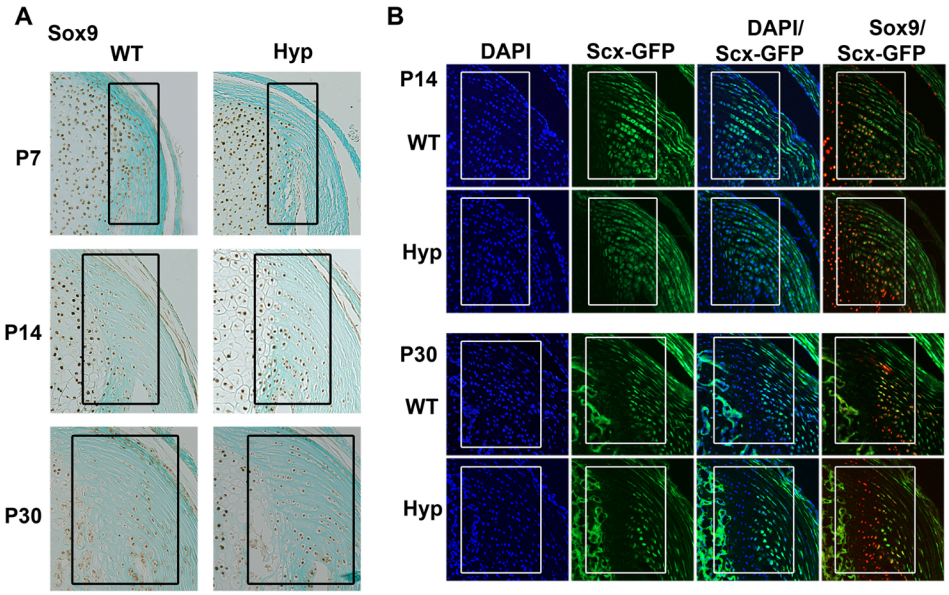

Fig. 4. Proximal enthesis cells in P30 Hyp mice exhibit persistent and enhanced Sox9 expression. (A) Immunohistochemistry for Sox9 (brown) in wild-type and Hyp entheses. Sections were counterstained with Fast Green. (B) Entheses from P14 and P30 wild-type and Hyp mice expressing scleraxis-GFP (Scx-GFP) (green). Sox9 immunofluorescence staining (red) in the entheses of Scx-GFP wild-type and Hyp mice. The enthesis region is outlined with a black or white box. Data are representative of three mice per genotype/treatment group.

Development (2018) 145, dev163519. doi:10.1242/dev.163519

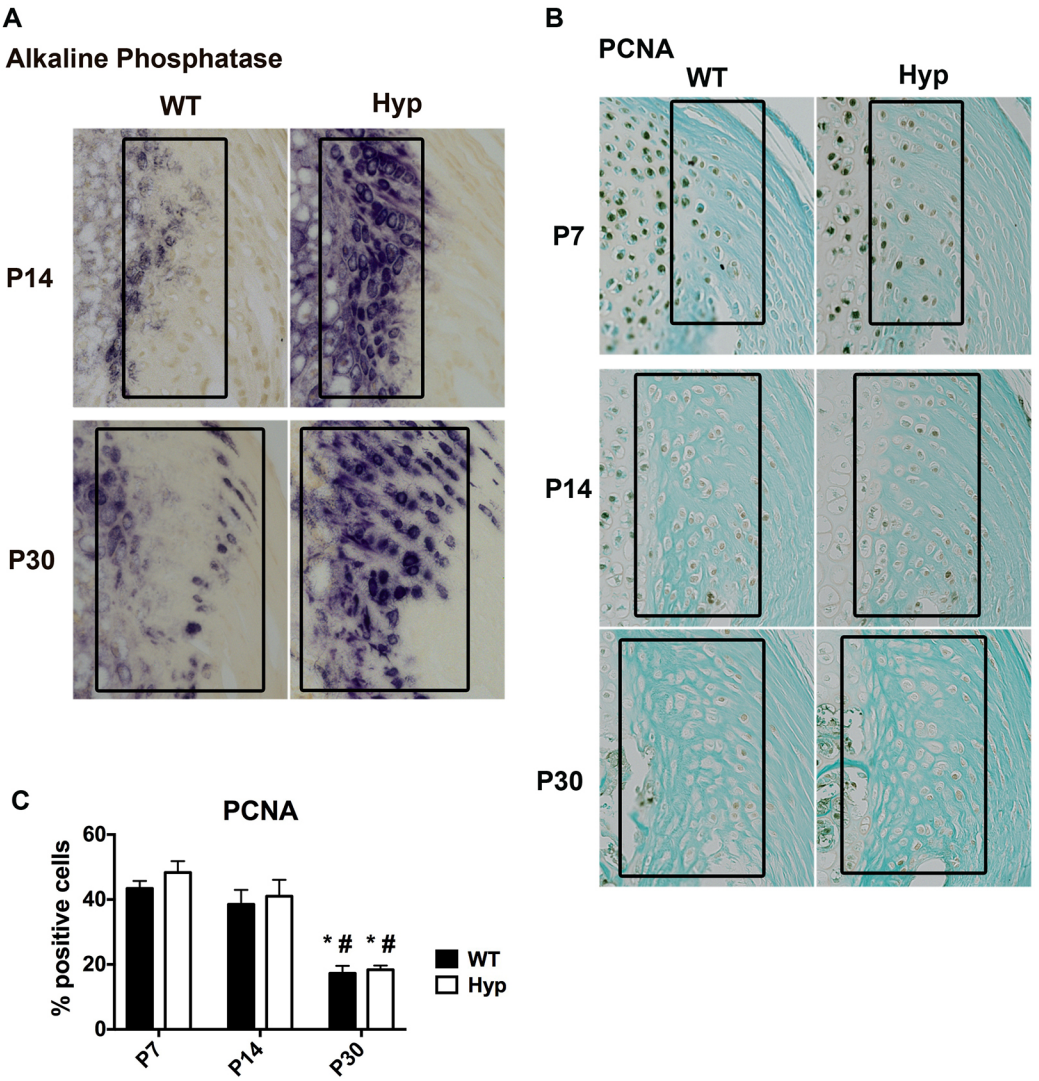

Fig. 5. Hyp entheses have increased alkaline phosphatase activity but do not have increased proliferation. (A) Alkaline phosphatase staining (purple) of entheses from P14 and P30 wild-type and Hyp mice. (B) Immunohistochemistry for PCNA in wild-type and Hyp entheses. Sections were counterstained with Fast Green. The enthesis region is outlined with a black box. (C) Percentage of PCNA-positive cells in wild-type and Hyp entheses. Data are representative of three mice per genotype group (mean±s.e.m.). **P*<0.05 versus P7, #*P*<0.05 versus P14.

Minina et al., 2001). BMP signaling is also necessary for the formation of the bony ridge onto which tendons insert (Blitz et al., 2009). Previous studies have shown that IHH signaling is crucial for the postnatal development of the enthesis, as ablation of the IHH target Smoothened from cells that express Scx disrupts the formation of fibrocartilage at the tendon-bone attachment site (Liu et al., 2013).

The current investigations characterize the time course of Hyp enthesopathy development postnatally, with Hyp entheses having increased expression of targets of BMP and IHH signalling at P14 followed by an expansion of hypertrophic Safranin O- and Sox9-positive cells in the proximal enthesis region by P30. These results therefore support the pathogenic role of BMP and IHH signaling in fibrocartilage development in XLH enthesopathy. Similar to Hyp enthesopathy, inflammatory enthesitis in mice and humans with ankylosing spondylitis is characterized by increased p-Smad1/5/9 immunoreactivity in affected entheses (Lories et al., 2005). Like Hyp enthesopathy, this alternate model of enthesis pathology supports the importance of BMP signaling in the pathophysiology of mineralizing enthesopathy. Lineage-tracing experiments demonstrated that fibrocartilage enthesis cells are descendants of $GDF5^{+}$ precursors (Dyment et al., 2015) and the current investigations show that expression of GDF5 is increased in Hyp entheses, supporting a role for GDF5 in activating BMP signaling in Hyp entheses.

Our studies demonstrate that initiating 1,25D or FGF2Ab therapy prior to the development of enhanced BMP and IHH signaling in the Hyp entheses attenuates the development of enthesopathy. This contrasts with previous investigations demonstrating that treating of Hyp mice with 1,25D (three times per week) and oral phosphate supplementation starting at week 3 and continuing to week 12 does not alter alkaline phosphatase staining in the Hyp entheses (Karaplis et al., 2012). This disparity suggests that, once established, enthesopathy does not regress, or that phosphate supplementation antagonizes the beneficial effects of 1,25D. Regardless, our findings have important implications for the treatment of children with XLH, supporting the beneficial effects of early, consistent and optimized 1,25D or FGF23Ab therapy to prevent the development of enthesopathies that cause pain and mobility issues in adults with XLH. A retrospective study failed to find a correlation between

Development (2018) 145, dev163519. doi:10.1242/dev.163519

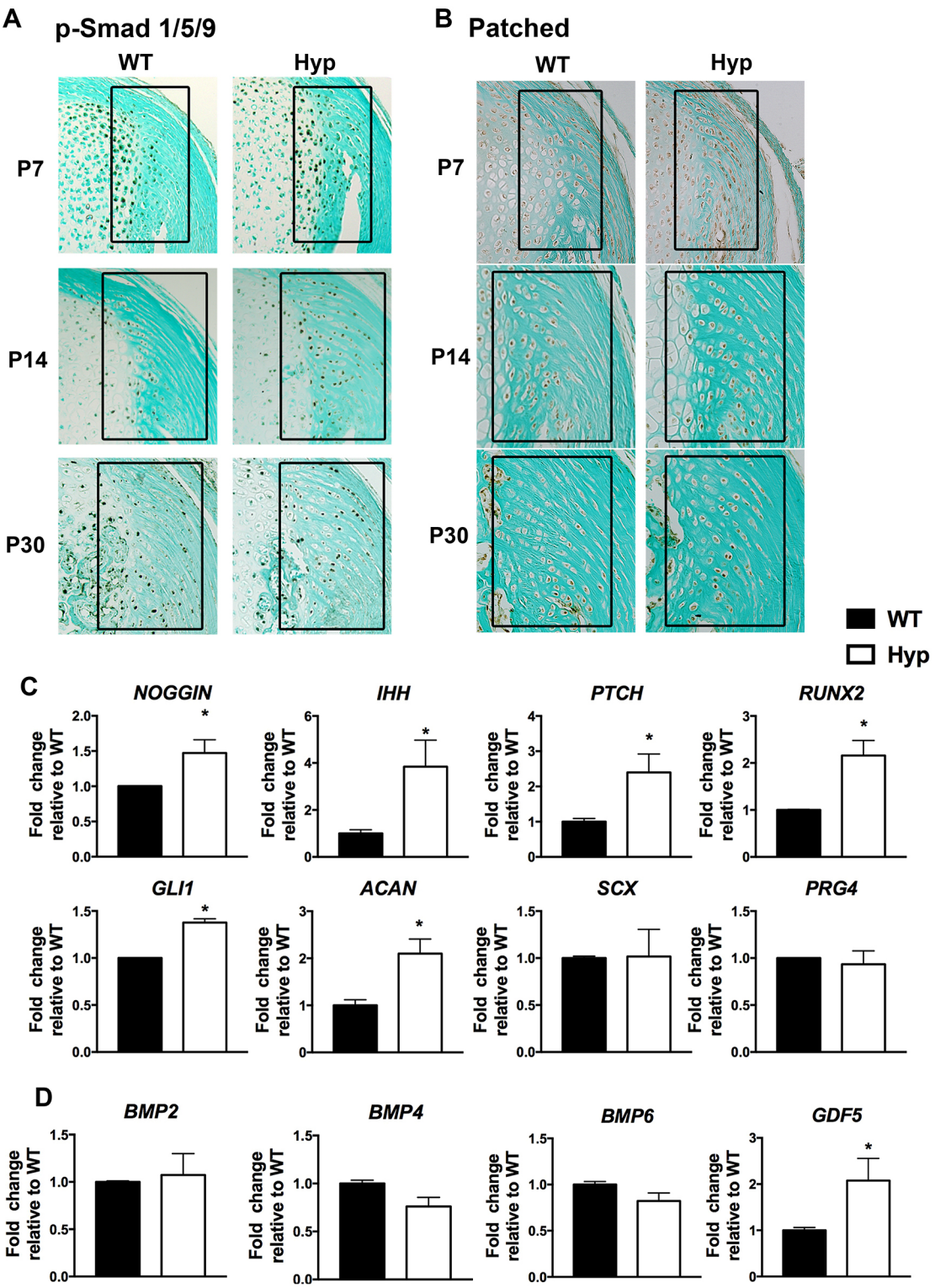

Fig. 6. Hyp entheses exhibit increased expression of BMP and IHH signaling target genes. (A,B) Immunohistochemistry for p-Smad1/5/9 (A) and patched (Ptch1) (B) in wild-type and Hyp entheses. The enthesis region is outlined with a black box. Sections were counterstained with Fast Green. Data are representative of three mice per age/genotype group. (C) mRNA expression of the BMP and IHH signaling target genes *Acan*, *Prg4* and *Scx* in P14 wild-type and Hyp entheses. Gene expression is normalized to that of wild type. (D) mRNA expression of BMP genes and *Gdf5* in P14 wild-type and Hyp entheses. Gene expression is normalized to that of wild type. Data are representative of three mice per age/genotype group (mean±s.e.m.). **P*<0.05 versus wild type.

enthesopathy and length of lifetime spent taking phosphate and 1,25D therapy in XLH patients (Connor et al., 2015). It is possible that beneficial effects were not observed due to lack of optimization of 1,25D therapy (Liu et al., 2016), delay and/or inconsistent therapy, or the possibility that phosphate supplementation prevents the beneficial effects of 1,25D.

Development (2018) 145, dev163519. doi:10.1242/dev.163519

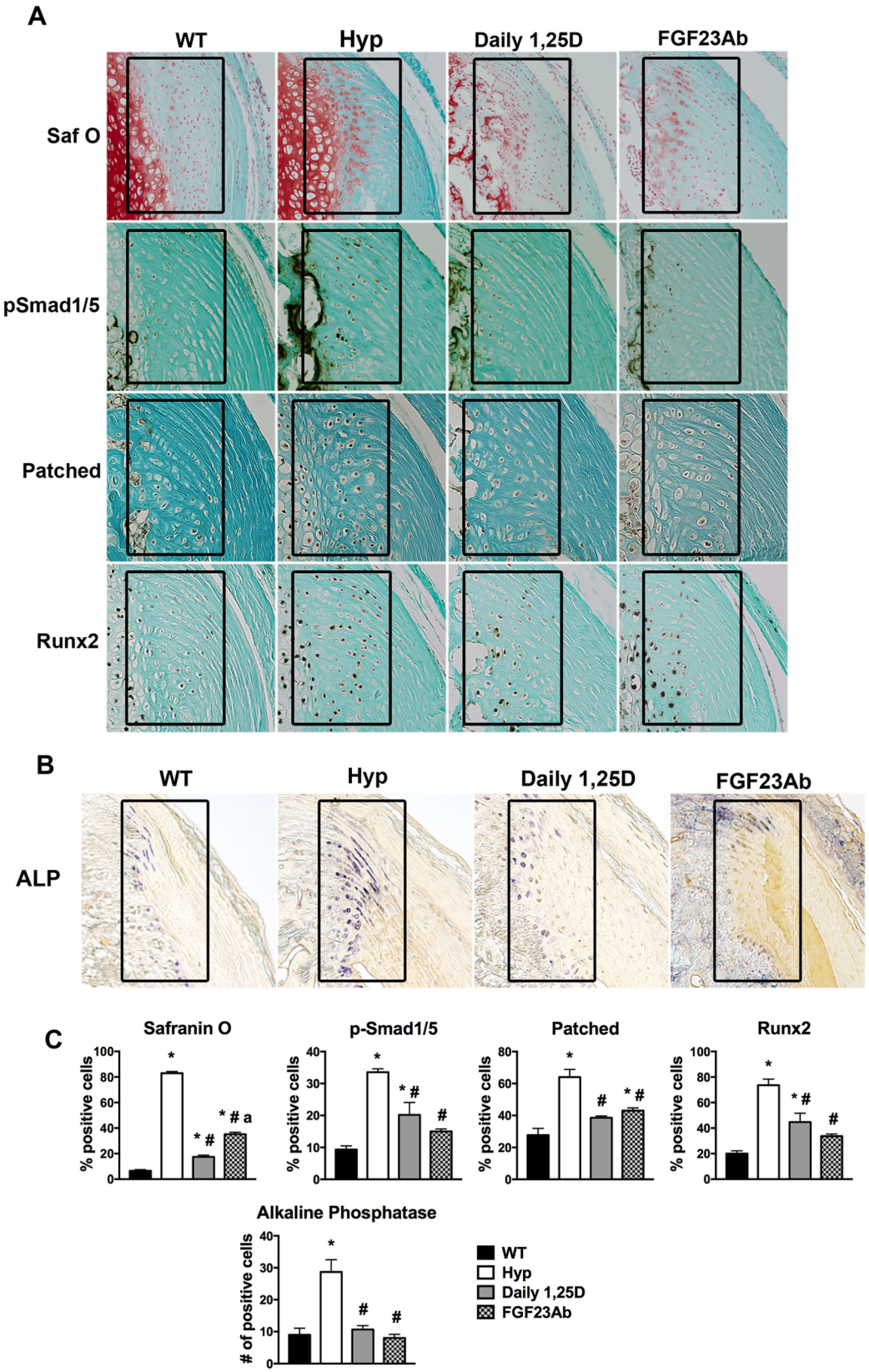

Fig. 7. Treatment of Hyp mice with 1,25D or FGF23Ab attenuates enthesopathy. (A) Safranin O staining (red) and p-Smad1/5/9, Ptch1 and Runx2 immunohistochemistry was performed on entheses from P30 wild-type and Hyp control mice and Hyp mice treated with 1,25D or FGF23Ab. Sections were counterstained with Fast Green. (B) Alkaline phosphatase (purple) staining of entheses from P75 wild-type and Hyp control mice, and Hyp mice treated with 1,25D or FGF23Ab. The enthesis region is outlined with a black box. Data are representative of three mice per genotype/treatment group. (C) Quantitation of the percentage of Safranin O-positive cells immunoreactive for p-Smad1/5/9, Ptch1 and Runx2, and the percentage of alkaline phosphatase-positive cells (mean±s.e.m.). $^{*}P<0.05$ versus wild type, $^{\#}P<0.05$ versus Hyp, $^{a}P<0.05$ versus 1.25D.

Development (2018) 145, dev163519. doi:10.1242/dev.163519

Table 1. Serum parameters in Hyp mice treated with daily 1,25D or FGF23Ab

	Wild type	Hyp	Daily 1,25D	FGF23Ab
Ca (mg/dl)	10.2±0.7	9.6±0.1	10.3±0.2	9.4±0.2
Pi (mg/dl)	11.0±0.6	5.9±0.4*	7.9±0.3*,‡	6.5±0.2*,‡,§

Data are representative of three mice per genotype/treatment group (mean±s.e.m.).
Ca,serum calcium; Pi, serum phosphorus.
*P<0.05 versus WT, ‡P<0.05 versus Hyp Con, §P<0.05 versus Daily 1,25D.

Several pathological states with increased serum levels of FGF23, including transgenic mice overexpressing FGF23 (Karaplis et al., 2012), humans lacking DMP1 (Mäkitie et al., 2010), and mice and humans with XLH (Liang et al., 2009), exhibit enthesopathy, suggesting that enhanced FGF23 action plays a role in the pathogenesis of enthesopathy in XLH. However, based on our findings that treatment with 1,25D dramatically increased expression of FGF23 (Liu et al., 2016), yet prevented the enthesopathy in Hyp mice, it is unlikely that increased FGF23 action plays a major pathogenic role. Rather, the inhibition of BMP signaling seen in 1,25D-treated chondrocytes, data showing that 1,25D inhibits BMP expression *in vitro* (Virdi et al., 1998; Fu et al., 2013) and the enhanced expression of IHH target genes in keratinocytes lacking the VDR (Lisse et al., 2014) all suggest that impaired 1,25D action underlies the enhanced BMP and IHH signaling in the entheses of Hyp mice. Thus, the current investigations implicate hypophosphatemia and/or decreased 1,25D action in the pathogenesis of enthesopathy in XLH.

MATERIALS AND METHODS

Study design

The purpose of these studies is to characterize the phenotype of the enthesopathy observed in Hyp mice with XLH. Lineage-tracing studies were performed to determine the origin of the abnormal cells observed in Hyp entheses. Immunohistochemical, histological and gene expression analyses were performed to identify markers and signaling pathways that are aberrantly expressed in the Hyp entheses. To examine whether improving phosphate and 1,25D homeostasis or blocking FGF23 action prevents the development of Hyp enthesopathy, Hyp mice were treated with 1,25D or an anti-FGF23 blocking antibody (FGF23Ab).

Animal studies

Animal studies were approved by the Massachusetts General Hospital Institutional Animal Care and Use Committee. All mice were on a C57BL/6J background, maintained in a virus- and parasite-free barrier facility, and exposed to a 12 h light/dark cycle. Mice were weaned at P18 onto house chow (1% calcium, 0.6% phosphate) and housed at up to five mice per cage.

Male and female wild-type, Hyp, Scx-GFP (Pryce et al., 2007), Sox9-CreERT2 (Soeda et al., 2010), Scx-Cre (Blitz et al., 2009), Scx-CreERT2 (Howell et al., 2017) and Rosa26-loxP-stop-loxP-TdTomato ($R26R^{Tom}$ mice, JAX 7914) mice were studied. Scx-GFP mice were crossed to Hyp mice to examine Scx expression in entheses of wild-type and Hyp mice. The Scx-Cre, Sox9-CreERT and Scx-CreERT2 mice were crossed to the $R26R^{Tom}$ mice, and the resultant Scx-Cre; $R26R^{Tom}$, Sox9-CreERT2; $R26R^{Tom}$ and Scx-CreERT2; $R26R^{Tom}$ mice were mated to the Hyp mice. For lineage-tracing experiments using the Sox9-CreERT2 and Scx-CreERT2 mice, intraperitoneal injections of tamoxifen (0.1 mg/g, Sigma) dissolved in sunflower oil were performed at P2. Tamoxifen-injected Sox9-CreERT2 mice were sacrificed on P5, P14 and P30, and tamoxifen-injected Scx-CreERT2 mice were sacrificed at P14.

Male and female Hyp mice were injected daily with 1,25D (175 pg/g/day, Akorn) or three times per week with FGF23Ab (35 µg/g, Amgen) starting on P2. Wild-type and Hyp control littermates of both sexes received vehicle or isotype-matched antibody (35 µg/g).

Histology

The Achilles tendon entheses were dissected from mice, fixed in 10% formalin/PBS, decalcified in 20% EDTA/PBS (pH 8.0) and paraffin wax embedded sections were prepared. For frozen sections, decalcified entheses were embedded in OCT and cryosectioned at 5 µm. Immunofluroescent images were captured with an epifluoresence microscope (Nikon Eclipse E800) with prefigured triple band filter settings for DAPI/FITC/TRITC.

To evaluate alkaline phosphatase activity, P75 entheses were fixed in 70% alcohol and processed for resin-embedded sectioning. P5, P14 and P30 entheses were fixed in 10% formalin and processed as for frozen sections. Deplasticized or frozen sections were immersed in Tris Buffer (pH 9.4) for 1 h and then incubated in alkaline phosphate staining solution [Tris buffer (pH 9.4), Fast Blue solution, Napthol ASBI Phosphate solution and magnesium chloride] at room temperature.

Immunohistochemistry

Paraffin sections were rehydrated and blocked with TNB [0.1 M Tris-HCl (pH 7.5), 0.15 M NaCl, 0.5% blocking reagent (Perkin Elmer)]. For Sox9 immunohistochemistry, antigen retrieval was performed by incubating with trypsin (Sigma) at 37°C, whereas for p-Smad1/5/9 and Runx2 immunohistochemistry, sections were incubated with proteinase K at 37°C. After incubation with primary antibody [anti-Sox9 antibody (1:2000, Millipore, AB5535), anti-p-Smad1/5/9 antibody (1:100, Cell Signaling, 13820) or anti-Runx2 antibody (1:800, Cell Signaling, 12556)], signal detection was performed using biotinylated goat-anti rabbit secondary antibody (Vector) followed by amplification with the TSA Kit (Perkin Elmer). For Ptch1 immunohistochemistry, paraffin sections were subjected to antigen retrieval with trypsin and blocked with 10% heat-inactivated fetal bovine serum (hi-FBS) in PBS. Following incubation with anti-Ptch1 antibody (1:300, AbCam, ab53715), signal was detected using a goat anti-rabbit HRP antibody (Sigma). For proliferating cell nuclear antigen (PCNA) immunohistochemistry, paraffin sections were blocked with 10% hi-FBS in PBS, then incubated with anti-PCNA antibody (1:100, Thermo-Fisher Scientific, 13-3900). Signal was detected using a biotinylated goat anti-mouse secondary antibody (Vector) followed by incubation with streptavidin-conjugated horseradish peroxidase (Perkin Elmer).

For Sox9 immunohistochemistry on frozen sections, sections were equilibrated to room temperature, blocked with 10% hi-FBS/PBS and incubated with anti-Sox9 antibody (1:250). Fluorescent signal was detected using Alexa-Fluor 546-conjugated donkey anti-rabbit antibody (Invitrogen).

The number of alkaline phosphatase-positive, the percentage Safranin O- or Scx-Tomato-positive and the percentage of immunoreactive cells in the entheses were quantitated. The enthesis region was defined on one side by the distal border of the calcaneal secondary ossification center and on the other end by the point where the anterior part of the tendon emerges from the articular surface. The ratio of the number of immunoreactive, Safranin O-positive or Scx-Tomato-positive cells to the total number of cells in the defined enthesis region was calculated.

Enthesis RNA analysis

The site at which the P14 wild-type and Hyp Achilles tendon insert into the calcaneus was identified under a dissection microscope (Nikon) at 5× magnification and isolated using a microsurgical knife by slicing through the proximal end of the tendon and the region adjacent to the distal part of the calcaneus. The enthesis tissue was homogenized in Trizol (Thermo Fisher Scientific). Total RNA was precipitated using 100% ethanol and purified using the PureLink RNA mini kit (Thermo Fisher Scientific).

In vitro chondrocyte studies

Primary chondrocytes were isolated from P2 wild-type murine ribs and cultured as previously described (Sabbagh et al., 2005). Chondrocytes cultured for 48 h were serum restricted (0.5% FBS) and treated with 10^{-8} M 1,25D for 18 h prior to exposure to recombinant human BMP2 (rhBMP2) (150 ng/ml) for 4 h. Chondrocytes were harvested after 72 h in culture for isolation of RNA using a PureLink RNA mini kit (Thermo Fisher Scientific).

Development (2018) 145, dev163519. doi:10.1242/dev.163519

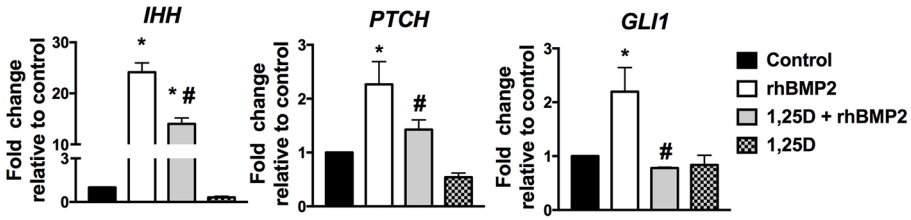

Fig. 8. 1,25D treatment of chondrogenic cells inhibits BMP-induced IHH signaling. Primary murine chondrocytes treated with 150 ng/ml of recombinant human BMP2 with or without pretreatment with 10^{-8}M 1,25D. Gene expression analysis performed for *Ihh*, *Ptch1* and *Gli1*. Data are representative of those obtained from three experiments (mean±s.e.m.). **P*<0.05 versus control, #*P*<0.05 versus hrBMP2.

Gene expression analyses

RNA was reverse transcribed with PrimeScript (Takara-Clontech). Quantitative real time-PCR was performed using the QuantiTect SYBR Green RT-PCR kit (Qiagen) on an Opticon DNA engine (MJ Research). Gene expression was normalized to that of a control gene for each sample, using the methods of Livak and Schmittgen (Miedlich et al., 2010).

Serum parameters

Serum calcium and phosphate were measured using a HESKA DRI CHEM 7000 veterinary analyzer (Liu et al., 2016).

Statistical analysis

All data shown are reported as mean±s.e.m.. Student's two-tailed *t*-test was used to determine significance between wild-type and Hyp groups. One-way ANOVA followed by Fisher's least significant difference (LSD) test was used to analyze significance between all control and 1,25D- or FGF23Ab-treated groups. Significance was defined as $P<0.05$. GraphPad Prism software was used for all data analysis.

Competing interests

The authors declare no competing or financial interests.

Author contributions

Conceptualization: E.S.L., M.B.D.; Methodology: E.S.L., J.S.M., W.Z., M.B.D.; Validation: E.S.L.; Formal analysis: E.S.L.; Investigation: E.S.L., J.S.M., W.Z.; Writing - original draft: E.S.L.; Writing - review & editing: E.S.L., M.B.D.; Visualization: E.S.L.; Supervision: E.S.L., M.B.D.; Project administration: E.S.L., M.B.D.; Funding acquisition: E.S.L., M.B.D.

Funding

This work was supported by grants from the National Institutes of Health (K08 AR067854 to E.S.L., R01 AR061376 and R01 AR072650 to M.B.D., and P30 AR061313). Deposited in PMC for release after 12 months.

References

Akiyama, H., Kim, J.-E., Nakashima, K., Balmes, G., Iwai, N., Deng, J. M., Zhang, Z., Martin, J. F., Behringer, R. R., Nakamura, T. et al. (2005). Osteo-chondroprogenitor cells are derived from Sox9 expressing precursors. *Proc. Natl. Acad. Sci. USA* **102**, 14665-14670.

Bi, W., Deng, J. M., Zhang, Z., Behringer, R. R. and de Crombrugghe, B. (1999). Sox9 is required for cartilage formation. *Nat. Genet.* **22**, 85-89.

Blitz, E., Viukov, S., Sharir, A., Shwartz, Y., Galloway, J. L., Pryce, B. A., Johnson, R. L., Tabin, C. J., Schweitzer, R. and Zelzer, E. (2009). Bone ridge patterning during musculoskeletal assembly is mediated through SCX regulation of Bmp4 at the tendon-skeleton junction. *Dev. Cell* **17**, 861-873.

Blitz, E., Sharir, A., Akiyama, H. and Zelzer, E. (2013). Tendon-bone attachment unit is formed modularly by a distinct pool of Scx- and Sox9-positive progenitors. *Development* **140**, 2680-2690.

Carpenter, T. O., Imel, E. A., Holm, I. A., Jan de Beur, S. M. and Insogna, K. L. (2011). A clinician's guide to X-linked hypophosphatemia. *J. Bone Miner Res.* **26**, 1381-1388.

Chen, X., Macica, C. M., Dreyer, B. E., Hammond, V. E., Hens, J. R., Philbrick, W. M. and Broadus, A. E. (2006). Initial characterization of PTH-related protein gene-driven lacZ expression in the mouse. *J. Bone Miner Res.* **21**, 113-123.

Connor, J., Olear, E. A., Insogna, K. L., Katz, L., Baker, S., Kaur, R., Simpson, C. A., Sterpka, J., Dubrow, R., Zhang, J. H. et al. (2015). Conventional therapy in adults with x-linked hypophosphatemia: effects on enthesopathy and dental disease. *J. Clin. Endocrinol. Metab.* **100**, 3625-3632.

Dyment, N. A., Breidenbach, A. P., Schwartz, A. G., Russell, R. P., Aschbacher-Smith, L., Liu, H., Hagiwara, Y., Jiang, R., Thomopoulos, S., Butler, D. L. et al. (2015). Gdf5 progenitors give rise to fibrocartilage cells that mineralize via hedgehog signaling to form the zonal enthesis. *Dev. Biol.* **405**, 96-107.

Fu, B., Wang, H., Wang, J., Barouhas, I., Liu, W., Shuboy, A., Bushinsky, D. A., Zhou, D. and Favus, M. J. (2013). Epigenetic regulation of BMP2 by 1,25-dihydroxyvitamin D3 through DNA methylation and histone modification. *PLoS ONE* **8**, e61423.

Genin, G. M., Kent, A., Birman, V., Wopenka, B., Pasteris, J. D., Marquez, P. J. and Thomopoulos, S. (2009). Functional grading of mineral and collagen in the attachment of tendon to bone. *Biophys. J.* **97**, 976-985.

Grimsrud, C. D., Romano, P. R., D'Souza, M., Puzas, J. E., Schwarz, E. M., Reynolds, P. R., Roiser, R. N. and O'Keefe, R. J. (2001). BMP signaling stimulates chondrocyte maturation and the expression of Indian hedgehog. *J. Orthop. Res.* **19**, 18-25.

Holm, I. A., Huang, X. and Kunkel, L. M. (1997). Mutational analysis of the PEX gene in patients with X-linked hypophosphatemic rickets. *Am. J. Hum. Genet.* **60**, 790-797.

Howell, K., Chien, C., Bell, R., Laudier, D., Tufa, S. F., Keene, D. R., Andarawis-Puri, N. and Huang, A. H. (2017). Novel model of tendon regeneration reveals distinct cell mechanisms underlying regenerative and fibrotic tendon healing. *Sci. Rep.* **7**, 45238.

Jonsson, K. B., Zahradnik, R., Larsson, T., White, K. E., Sugimoto, T., Imanishi, Y., Yamamoto, T., Hampson, G., Koshiyama, H., Ljunggren, O. et al. (2003). Fibroblast growth factor 23 in oncogenic osteomalacia and X-linked hypophosphatemia. *N Engl. J. Med.* **348**, 1656-1663.

Karaplis, A. C., Bai, X., Falet, J.-P. and Macica, C. M. (2012). Mineralizing enthesopathy is a common feature of renal phosphate-wasting disorders attributed to FGF23 and is exacerbated by standard therapy in hyp mice. *Endocrinology* **153**, 5906-5917.

Killian, M. L. and Thomopoulos, S. (2016). Scleraxis is required for the development of a functional tendon enthesis. *FASEB J.* **30**, 301-311.

Kobayashi, T., Lyons, K. M., McMahon, A. P. and Kronenberg, H. M. (2005). BMP signaling stimulates cellular differentiation at multiple steps during cartilage development. *Proc. Natl. Acad. Sci. USA* **102**, 18023-18027.

Kronenberg, H. M. (2003). Developmental regulation of the growth plate. *Nature* **423**, 332-336.

Kumar, M., Ray, P. and Chapman, S. C. (2012). Fibroblast growth factor and bone morphogenetic protein signaling are required for specifying prechondrogenic identity in neural crest-derived mesenchyme and initiating the chondrogenic program. *Dev. Dyn.* **241**, 1091-1103.

Liang, G., Katz, L. D., Insogna, K. L., Carpenter, T. O. and Macica, C. M. (2009). Survey of the enthesopathy of X-linked hypophosphatemia and its characterization in Hyp mice. *Calcif. Tissue Int.* **85**, 235-246.

Lisse, T. S., Saini, V., Zhao, H., Luderer, H. F., Gori, F. and Demay, M. B. (2014). The vitamin D receptor is required for activation of cWnt and hedgehog signaling in keratinocytes. *Mol. Endocrinol.* **28**, 1698-1706.

Liu, S., Zhou, J., Tang, W., Jiang, X., Rowe, D. W. and Quarles, L. D. (2006). Pathogenic role of Fgf23 in Hyp mice. *Am J Physiol Endocrinol Metab.* **291**, E38-E49.

Liu, C.-F., Aschbacher-Smith, L., Barthelery, N. J., Dyment, N., Butler, D. and Wylie, C. (2012). Spatial and temporal expression of molecular markers and cell signals during normal development of the mouse patellar tendon. *Tissue Eng. Part A* **18**, 598-608.

Liu, C.-F., Breidenbach, A., Aschbacher-Smith, L., Butler, D. and Wylie, C. (2013). A role for hedgehog signaling in the differentiation of the insertion site of the patellar tendon in the mouse. *PloS ONE* **8**, e65411.

Liu, E. S., Martins, J. S., Raimann, A., Chae, B. T., Brooks, D. J., Jorgetti, V., Bouxsein, M. L. and Demay, M. B. (2016). 1,25-Dihydroxyvitamin D alone improves skeletal growth, microarchitecture and strength in a murine model of XLH, despite enhanced FGF23 expression. *J. Bone Miner. Res.* **31**, 929-939.

Lories, R. J. U., Derese, I. and Luyten, F. P. (2005). Modulation of bone morphogenetic protein signaling inhibits the onset and progression of ankylosing enthesitis. *J. Clin. Invest.* **115**, 1571-1579.

Mäkitie, O., Pereira, R. C., Kaitila, I., Turan, S., Bastepe, M., Laine, T., Kroger, H., Cole, W. G. and Juppner, H. (2010). Long-term clinical outcome and carrier phenotype in autosomal recessive hypophosphatemia caused by a novel DMP1 mutation. *J. Bone Miner. Res.* **25**, 2165-2174.

Miedlich, S. U., Zalutskaya, A., Zhu, E. D. and Demay, M. B. (2010). Phosphate-induced apoptosis of hypertrophic chondrocytes is associated with a decrease in mitochondrial membrane potential and is dependent upon ERK1/2 phosphorylation. *J. Biol. Chem.* **285**, 18270-18275.

Minina, E., Wenzel, H. M., Kreschel, C., Karp, S., Gaffield, W., McMahon, A. P. and Vortkamp, A. (2001). BMP and Ihh/PTHrP signaling interact to coordinate chondrocyte proliferation and differentiation. *Development* **128**, 4523-4534.

Murchison, N. D., Price, B. A., Conner, D. A., Keene, D. R., Olson, E. N., Tabin, C. J. and Schweitzer, R. (2007). Regulation of tendon differentiation by scleraxis distinguishes force-transmitting tendons from muscle-anchoring tendons. *Development* **134**, 2697-2708.

Pryce, B. A., Brent, A. E., Murchison, N. D., Tabin, C. J. and Schweitzer, R. (2007). Generation of transgenic tendon reporters, ScxGFP and ScxAP, using regulatory elements of the scleraxis gene. *Dev. Dyn.* **236**, 1677-1682.

Sabbagh, Y., Carpenter, T. O. and Demay, M. B. (2005). Hypophosphatemia leads to rickets by impairing caspase-mediated apoptosis of hypertrophic chondrocytes. *Proc. Natl. Acad. Sci.* **102**, 9637-9642.

Schwartz, A. G., Pasteris, J. D., Genin, G. M., Daulton, T. L. and Thomopoulos, S. (2012). Mineral distributions at the developing tendon enthesis. *PLoS ONE* **7**, e48630.

Schwartz, A. G., Long, F. and Thomopoulos, S. (2015). Enthesis fibrocartilage cells originate from a population of Hedgehog-responsive cells modulated by the loading environment. *Development* **142**, 196-206.

Schweitzer, R., Chyung, J. H., Murtaugh, L. C., Brent, A. E., Rosen, V., Olson, E. N., Lassar, A. and Tabin, C. J. (2001). Analysis of the tendon cell fate using Scleraxis, a specific marker for tendons and ligaments. *Development* **128**, 3855-3866.

Seki, K. and Hata, A. (2004). Indian hedgehog gene is a target of the bone morphogenetic protein signaling pathway. *J. Biol. Chem.* **279**, 18544-18549.

Soeda, T., Deng, J. M., de Crombrugghe, B., Behringer, R. R., Nakamura, T. and Akiyama, H. (2010). Sox9-expressing precursors are the cellular origin of the cruciate ligament of the knee joint and the limb tendons. *Genesis* **48**, 635-644.

St-Jacques, B., Hammerschmidt, M. and McMahon, A. P. (1999). Indian hedgehog signaling regulates proliferation and differentiation of chondrocytes and is essential for bone formation. *Genes Dev.* **13**, 2072-2086.

Sugimoto, Y., Takimoto, A., Akiyama, H., Kist, R., Scherer, G., Nakamura, T., Hiraki, Y. and Shukunami, C. (2013). Scx+/Sox9+ progenitors contribute to the establishment of the junction between cartilage and tendon/ligament. *Development* **140**, 2280-2288.

Sugita, D., Yayama, T., Uchida, K., Kokubo, Y., Nakajima, H., Yamagishi, A., Takeura, N. and Baba, H. (2013). Indian hedgehog signaling promotes chondrocyte differentiation in enchondral ossification in human cervical ossification of the posterior longitudinal ligament. *Spine* **38**, E1388-E1396.

Thomopoulos, S., Genin, G. M. and Galatz, L. M. (2010). The development and morphogenesis of the tendon-to-bone insertion - what development can teach us about healing. *J. Musculoskelet. Neuronal. Interact.* **10**, 35-45.

Virdi, A. S., Cook, L. J., Oreffo, R. O. and Triffitt, J. T. (1998). Modulation of bone morphogenetic protein-2 and bone morphogenetic protein-4 gene expression in osteoblastic cell lines. *Cell. Mol. Biol. (Noisy-le-grand)* **44**, 1237-1246.

Zelzer, E., Blitz, E., Killian, M. L. and Thomopoulos, S. (2014). Tendon-to-bone attachment: from development to maturity. *Birth Defects Res. C Embryo Today* **102**, 101-112.